Bioresource Technology 147 (2013) 605–613

Contents lists available at ScienceDirect

Bioresource Technology

journal homepage: www.elsevier.com/locate/biortech

Kinetic modeling of batch fermentation for *Populus* hydrolysate tolerant mutant and wild type strains of *Clostridium thermocellum*

Jessica L. Linville [a,b], Miguel Rodriguez Jr. [b,c], Jonathan R. Mielenz [b,c], Chris D. Cox [a,b,d,*]

[a] Department of Civil and Environmental Engineering, University of Tennessee, Knoxville, TN, United States
[b] Bioenergy Science Center, Oak Ridge National Laboratory, Oak Ridge, TN, United States
[c] Biosciences Division, Oak Ridge National Laboratory, Oak Ridge, TN, United States
[d] Center for Environmental Biotechnology, University of Tennessee, Knoxville, TN, United States

HIGHLIGHTS

- Analyzed a *Populus* hydrolysate mutant and wild type strain of *Clostridium thermocellum*.
- Used a Monod based kinetic model for growth with and without *Populus* hydrolysate.
- *Populus* mutant had a faster growth rate and was less inhibited than wild type.
- *Populus* mutant is more tolerant to individual inhibitors than the wild type.
- *Populus* mutant has a lower ability to detoxify the hydrolysate than wild type.

ARTICLE INFO

Article history:
Received 19 June 2013
Received in revised form 12 August 2013
Accepted 13 August 2013
Available online 20 August 2013

Keywords:
Clostridium thermocellum
Populus hydrolysate
Kinetic model
Inhibition
Biofuels

ABSTRACT

The extent of inhibition of two strains of *Clostridium thermocellum* by a *Populus* hydrolysate was investigated. A Monod-based model of wild type (WT) and *Populus* hydrolysate tolerant mutant (PM) strains of the cellulolytic bacterium *C. thermocellum* was developed to quantify growth kinetics in standard media and the extent of inhibition to a *Populus* hydrolysate. The PM was characterized by a higher growth rate (μ_{max} = 1.223 vs. 0.571 h^{-1}) and less inhibition ($K_{I,gen}$ = 0.991 vs. 0.757) in 10% v/v *Populus* hydrolysate compared to the WT. In 17.5% v/v *Populus* hydrolysate inhibition of PM increased slightly ($K_{I,gen}$ = 0.888), whereas the WT was strongly inhibited and did not grow in a reproducible manner. Of the individual inhibitors tested, 4-hydroxybenzoic acid was the most inhibitory, followed by galacturonic acid. The PM did not have a greater ability to detoxify the hydrolysate than the WT.

1. Introduction

Lignocellulosic biomass provides an abundant and renewable energy source. Lignocellulosic biomass contains sugars polymerized in the form of cellulose and hemicelluloses, which can be liberated by hydrolysis, and subsequently fermented to ethanol by microorganisms, such as *Clostridium thermocellum* (Palmqvist and Hahn-Hagerdal, 2000a). *C. thermocellum* is a Gram-positive, anaerobic, thermophilic, cellulolytic bacterium that can rapidly solubilize biomass, use cellulose as the sole carbon and energy source, and is under development for biofuel production (Brown et al., 2011; Linville et al., submitted for publication; Riederer et al., 2011; Yu et al., 2012). *C. thermocellum*'s cellulolytic ability gives it an advantage over organisms that are currently used for bioethanol production (e.g., yeast and *Zymomonas*), which can only ferment nonpolymeric carbohydrates (Roberts et al., 2010; Williams et al., 2007). *C. thermocellum* produces a number of industrially important fermentation products in addition to ethanol, including acetic acid, formic acid, lactic acid, and hydrogen (Roberts et al., 2010).

However, rapid and efficient fermentation of the lignocellulosic biomass hydrolysate is a not yet achievable on an industrial scale. While progress has been made in optimizing pretreatment methods to yield higher yields of fermentable sugars (Shao and Lynd, 2013), inhibition of fermentation by a range of toxic compounds generated during steam pretreatment and hydrolysis (Palmqvist and Hahn-Hagerdal, 2000a) remains a challenge. Inhibitory compounds can be classified according to three main functional groups: weak acids, furan derivatives, and phenolic compounds (Palmqvist and Hahn-Hagerdal, 2000a). Xylose, mannose, acetic acid, and galactose are liberated from hemicelluloses, and glucose is liberated from cellulose (Palmqvist and Hahn-Hagerdal, 2000b).

* Corresponding author at: Department of Civil and Environmental Engineering, University of Tennessee, Knoxville, TN, United States.
E-mail address: ccox9@utk.edu (C.D. Cox).

0960-8524/$ - see front matter © 2013 Published by Elsevier Ltd.
http://dx.doi.org/10.1016/j.biortech.2013.08.086

Furans are the primary aromatic inhibitor formed from sugar degradation during pretreatment (Klinke et al., 2004). Xylose is further degraded to 2-furfural and hexose is degraded to 5-hydroxymethyl furfural (HMF) (Palmqvist and Hahn-Hagerdal, 2000b). Galacturonic acid is formed from the degradation of galactose. Phenolic compounds are generated from the partial breakdown of lignin. Vanillin and syringic acid are formed by the degradation of the guaiacylpropane units and syringyl propane units of lignin, respectively. In addition, 4-hydroxybenzoic acid constitutes a large fraction of the lignin-derived compounds in hydrolysates from hardwood poplar (Palmqvist and Hahn-Hagerdal, 2000b).

These compounds have potential inhibitory effects, which decreases the ethanol yield and growth rate of the microorganism (Palmqvist and Hahn-Hagerdal, 2000a,b). In order to obtain an economically feasible conversion process, reduction in the inhibitory effect of the toxic compounds is necessary (Klinke et al., 2004). Current detoxification methods include biological, physical, and chemical methods (Palmqvist and Hahn-Hagerdal, 2000a). Detoxification of pretreated hydrolysates has been shown to improve their fermentability; however, processing options that minimize inhibitor formation coupled with tolerant fermenting microorganisms will likely be more cost effective.

Mathematical modeling is a proven tool in the quantitative analysis of complicated processes such as fermentative growth (Huang and Wang, 2010). Mathematical models that accurately predict biochemical phenomena are essential since the model provides the basis for design, control, optimization and scale-up of process systems (Huang and Wang, 2010). Various approximate kinetic formulations have proven useful to predict the performance of biochemical conversion processes (Gnanapragasam et al., 2011). A kinetic Monod-based model has the ability to accurately describe cell growth and product formation rates (Gnanapragasam et al., 2011; Ljunggren et al., 2011). Such models can also be extended to include product and toxic compound inhibition (Bouguettoucha et al., 2011; Boyer et al., 1992; Huang and Wang, 2010). Monod based models can also be applied to complex systems, such as continuous stirred-tanks reactors and activated sludge, to determine optimum growth conditions (Song et al., 2011).

Improved tolerance to inhibitory compounds found in pretreated biomass hydrolysate should improve the fermentation process and increase economic feasibility of consolidated bioprocessing. Inhibitory compounds have been shown to reduce the rate of ethanol production and the overall yield in *C. thermocellum* (DOE/SC-0095, 2006; Pienkos and Zhang, 2009). The purpose of this study was to quantify the extent of inhibition caused by a *Populus* hydrolysate with respect to growth, cellobiose utilization, and ethanol production of a wild type (WT) and *Populus* hydrolysate tolerant mutant (PM) strain of *C. thermocellum* in batch culture using a Monod-based model. Studies of the growth on various concentrations of the full *Populus* hydrolysate and individual inhibitors in the hydrolysate were also included to determine the relative inhibitory effect of various compounds in the hydrolysate. Also, a study was conducted to determine if the increased growth of the PM strain of *C. thermocellum* was due to an improved ability to detoxify the hydrolysate.

2. Methods

2.1. Strain and culture conditions

Clostridium thermocellum ATCC 27405 was obtained from Prof. Herb Strobel, University of Kentucky collection and denoted as the wild type (WT) strain. A *Populus* hydrolysate tolerant strain (PM) was developed from the WT strain as described in (Linville et al., submitted for publication). In all experiments, the cells were grown in media for thermophilic clostridia (MTC) with a substrate loading of 5 g/L cellobiose. The media was composed of 0.336 g/L potassium chloride [KCl], 0.25 g/L ammonium chloride [NH_4Cl], 1.00 g/L magnesium sulfate heptahydrate [$MgSO_4{\cdot}7H_2O$], 1.70 g/L potassium phosphate [KH_2PO_4], 0.50 g/L MOPS [$C_7H_{14}NO_4S$], 0.15 g/L calcium chloride dihydrate [$CaCl_2{\cdot}2H_2O$], 1.75 g/L trisodium citrate dehydrate [$Na_3C_6O_7{\cdot}2H_2O$], 0.6 g/L urea [CH_4N_2O], 1.00 g/L L-cysteine HCl, 0.30 mg/L resazurin, 2.0 mL of 1000× MTC minerals and 1.25 mL of 50× MTC vitamins (Ozkan et al., 2001; Zhang and Lynd, 2003). All chemicals were reagent grade and obtained from Sigma (St. Louis, MO, USA), unless otherwise indicated. The inoculum culture was grown in Balch (Bellco Glass, Inc., Vineland, NJ) tubes containing 9.5 mL of 5 g/L cellobiose MTC and 0.5 mL of the frozen stock culture. Cultures were allowed to reach exponential growth phase by incubation at 58 °C and 100 rpm, diluted to an optical density (OD_{600}) of 0.250 using sterile, anaerobic Milli-Q water and injected into the test conditions with an inoculum size of 10% by volume (Linville et al., submitted for publication). Milled *Populus trichocarpa* hydrolysate was pretreated at the National Renewable Energy Lab (NREL) using a 20% w/w solid loading and dilute concentrations of H_2SO_4 at temperatures of 165–195 °C (Schell et al., 2003). Solids were removed by filtration. The *Populus* hydrolysate was adjusted to a pH of 7.0 using 50% w/w NaOH and filter sterilized before being added to the MTC media.

2.2. Fermentation

Batch fermentations were conducted in triplicate in 1.5 L Q-plus jacketed glass fermentors (Sartorius Stedim Biotech, Bohemia, NY) using a 1 L working volume of MTC medium at 58 °C and stirred at a rate of 300 rpm, with pH controlled to 7.0 using 3 N NaOH. Fermentors containing only 5 g/L cellobiose were sparged with a filtered 20% CO_2/80% N_2 gas mixture and vigorously agitated overnight, followed by addition of the remaining medium components and *Populus* hydrolysate. *Populus* hydrolysate was added to the fermentors at 0%, 10% or 17.5% v/v concentration. The fermentors were then sparged for an additional 4 h with a 20% CO_2/80% N_2 gas mixture. The inoculum was a bottle culture grown overnight (11–13 h) in 5 g/L cellobiose, diluted to an OD_{600} of 0.200 ± 0.013, and added as 10% v/v to inoculate the fermenters. Well-mixed 5 mL aliquots of culture were harvested at regular intervals. Cell growth was monitored based on an increase in the OD_{600} of the culture blanked against a sterile sample of the same concentration of *Populus* hydrolysate containing media that was stored in an incubator at 58 °C. The OD_{600} of the culture was measured in triplicate by a Spectramax Plus 384 spectrophotometer (Molecular Devices, Sunnyvale, CA). The corresponding dry cell weight was obtained from a calibration curve. Metabolite analysis was performed using HPLC. Metabolites were separated at a flow rate of 0.5 mL/min in 5 mM H_2SO_4 using an Aminex HPX-87H column (Bio-Rad Laboratories, Inc, Hercules, CA).

2.3. Parameter estimation

The lag time was determined from a plot of log(biomass) as a function of time and removed from the experimental data before parameter optimization. The lag time was the same for the WT and PM strains; 4 h in standard media and 6 h in *Populus* hydrolysate media. Ethanol concentrations during the exponential growth phase were adjusted to include the ethanol found in the water trap in proportion to mass of ethanol measured in solution at each time point. Model simulations were conducted in Matlab 7.10.0 (R2010a) (The Mathworks, Inc., Natick MA). The model parameters were optimized using simulated annealing to minimize the weighted least square errors for the biomass, substrate and

fermentation products at each time point of the experiment in standard media. In *Populus* hydrolysate media the weighted least square errors for furfural and 5-HMF were also minimized to determine values of the inhibitor biodegradation parameters.

2.4. Populus hydrolysate tolerance

The WT and PM strains were cultured in cellobiose MTC media containing 0%, 10%, 20%, and 30% v/v *Populus* hydrolysate in 25 mL Balch tubes. The OD_{600} of the culture was measured in triplicate by a Spectramax Plus 384 spectrophotometer (Molecular Devices, Sunnyvale, CA). The OD_{600} was blanked using a sterile sample of medium with the same concentration of *Populus* hydrolysate stored in the incubator with the samples. The OD_{600} was used to determine the increase in cell growth over time.

2.5. Individual inhibitor tolerance

The WT and PM strains were cultured in cellobiose MTC media containing a single inhibitor at a concentration equivalent to its concentration in 17.5% and 35% v/v *Populus* hydrolysate. The six individual inhibitors chosen were furfural, 5-hydroxymethlyfurfural, vanillin, syringic acid, galacturonic acid, and 4-hydroxybenzoic acid (Sigma–Aldrich Co., St. Louis, MO). In addition, the six inhibitors were combined at the appropriate concentrations to make a 17.5% and 35% v/v model hydrolysate. The preparation of individual inhibitor media and model hydrolysate media was the same as the *Populus* hydrolysate media above except the pH was not adjusted for the individual inhibitor media. Samples were taken at 12, 24, and 48 h for OD_{600} and product concentrations. Measurement of the OD_{600} of the culture and metabolite analysis was performed as described above.

2.6. Detoxification

The ability of the WT and PM strains to detoxify *Populus* hydrolysate was tested by conducting fermentation re-growth experiments in media obtained from previous fermentations. To produce the media for the re-growth experiments, the WT and PM strains were grown uninterrupted for 72 h in 17.5% v/v *Populus* hydrolysate with 5 g/L cellobiose-MTC media. The concentration of the metabolites and inhibitors were measured before ($T = 0$ h) and after ($T = 72$ h) growth by HPLC. Cells were removed from the liquid media after the 72 h growth period by 0.2 μm filtration. The concentration of sugars and inhibitors were adjusted for both the PM and WT detoxified liquids so that the concentrations were roughly the same in both media. Both the PM and WT were regrown in each of these detoxified media. Biological triplicate experiments were conducted except for the WT-WT which was conducted in duplicate because one of the series did not grow. Measurements of the OD_{600} of the culture and metabolite analysis were performed as described above.

3. Results and discussion

3.1. Modeling of fermentative growth

Batch fermentations were conducted in fermentors to compare the performance of the PM and WT *C. thermocellum* strains in different concentrations of *Populus* hydrolysate. The PM was grown in three test conditions: standard medium (0% v/v *Populus* hydrolysate), 10% v/v and 17.5% v/v *Populus* hydrolysate media. The WT was grown in two test conditions: standard medium and 10% v/v *Populus* hydrolysate medium. Attempts to grow the WT strain in the presence of 17.5% v/v *Populus* hydrolysate resulted in a severely inhibited and non-reproducible growth pattern (data not shown). Samples were taken at regular intervals from each fermentation unit based on their growth rate.

Most models of biochemical processes are empirical and based on Monod's equations (Huang and Wang, 2010). In this work, the Monod model as formulated below was used to fit the experimental results:

$$\frac{dX}{dt} = (\mu - k_D) * X \tag{1}$$

$$\frac{dS}{dt} = -\frac{\mu * X}{Y_{X/S}} \tag{2}$$

$$\frac{dP_E}{dt} = \frac{Y_{E/S} * \mu * X}{Y_{X/S}} \tag{3}$$

$$\frac{dP_A}{dt} = \frac{Y_{A/S} * \mu * X}{Y_{X/S}} \tag{4}$$

where X is the cell biomass concentration (g/L); μ is the specific growth rate (h^{-1}); k_D is the first-order cell decay constant (h^{-1}); S is the substrate concentration (g/L); P_E and P_A are the product concentrations of ethanol and acetate, respectively (g/L); and $Y_{X/S}$, $Y_{E/S}$ and $Y_{A/S}$ are the yields of biomass, ethanol, and acetate per unit substrate consumed, respectively (g/g). For growth in standard conditions, the specific growth rate is described by Monod's equation:

$$\mu = \mu_{\max} * \left(\frac{S}{k_s + S}\right) \tag{5}$$

where $\mu_{\max}$ is the maximum specific growth rate (h^{-1}), and k_S is the half saturation concentrations for substrate S (g/L) (Bouguettoucha et al., 2011; Huang and Wang, 2010). Ethanol inhibition was not included in the model since it has been shown that ethanol inhibition is not significant at ethanol concentrations below low 1 g/L (Baskaran et al., 1995) and including this process did not improve the model.The first-order cell decay constant, k_D, was estimated directly from the decay portion of the growth curves of each strain in standard conditions by:

$$k_D = \frac{\ln\left(\frac{X_{\max}}{X_{\text{final}}}\right)}{\Delta t} \tag{6}$$

where $X_{\max}$ is the maximum biomass concentration (g/L) and X_{final} is the biomass concentration at the final time point (g/L) and Δt is the difference in time between the two biomass concentrations (Fig. 1). The cell decay constant was calculated as 0.12 h^{-1} for both strains. The decay constant is of the same order as another model of *C. thermocellum* grown on crystalline cellulose (Avicel) (Holwerda and Lynd, 2013). Initial guesses of the five model parameters ($\mu_{\max}$, k_s, $Y_{X/S}$, $Y_{E/S}$, and $Y_{A/S}$) were determined by manual adjustment of the parameters to obtain a reasonable visual fit to the data. The maximum specific growth rate and the half saturation constant for the substrate can also be estimated by various linearization methods such as the Eadie–Hofstee diagram, Hanes–Woolf plot and Lineweaver–Burk plot (Shuler and Kargi, 2002). Of those, the Hanes–Woolf plot is the most accurate (Shuler and Kargi, 2002). The simulated annealing function in Matlab was used to optimize the parameters (P) by minimizing the weighted least square errors:

$$min\chi^2(P) = \sum_i \sum_j \left(\frac{(\bar{y_{i,j}} - f_j(y_i, P))}{\sigma_{i,j}}\right)^2 \tag{7}$$

where $\bar{y_{i,j}}$ is the averaged value, $f_j(y_i,P)$ is the calculated value, and $\sigma_{i,j}$ is the sample standard deviation of variable j at time point i (Marquardt, 1963). Values of $f_j(y_i,P)$ were calculated using the ode45 function in Matlab. The confidence interval and

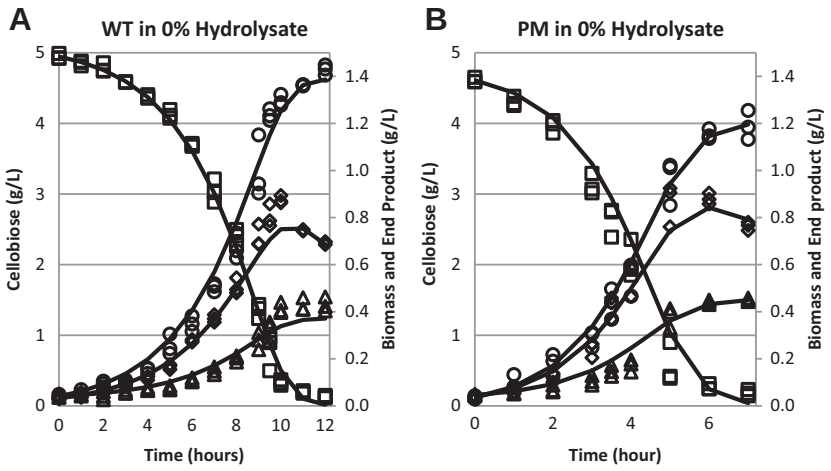

Fig. 1. Comparison of model-calculated and experimental results for the (A) WT in 0% v/v *Populus* hydrolysate and (B) PM in 0% v/v *Populus* hydrolysate for cellobiose utilization ([]), biomass formation (◇), and ethanol (Δ), and acetic acid (o) production. Experimental data are represented by points; model results are represented by solid lines.

codependence of each variable were determined from the covariance matrix. Derivative terms in the covariance matrix were determined numerically.

The optimized parameters and the 95% confidence intervals for both strains in standard media are shown in Table 1. The optimal model-calculated profiles for the WT and PM strains can be seen in Fig. 1. The model was able to accurately describe most of the variance found in the data as evidenced by the R^2 values of the entire system (Table 1). The model parameters suggest that the PM mutant has twice the specific growth rate, μ_{max}, which could be due to the mutation in the Spo0A homologue (Cthe_3087) (Linville et al., submitted for publication). Spo0A mutants, which are unable to go into sporulation, are thought to be locked in exponential growth since they continue to grow under nutritional conditions that would normally induce sporulation. Essentially they appear to maintain growth until the nutrients are exhausted, whereupon cell lysis occurs (Hoch, 1993). The PM has a mutation in the non-coding region 127 bp upstream of the first gene in the operon (Cthe_2602-09) which codes for the ATPase complex (Linville et al., submitted for publication). The ATPase is believed to help with the electron flux in the cell by pumping protons across the cell membrane (Raman et al., 2011). The mutation in the ATPase may also be a contributing factor to the increased growth rate of the PM. The biomass yield, $Y_{X/S}$, is similar between the two strains and similar to a recent model of *C. thermocellum* grown on crystalline cellulose (Avicel) (Holwerda and Lynd, 2013). The yield is also approximately 10-times as great as hydrogen producing strains of Clostridia (Song et al., 2011). This further suggests that the increased tolerance is due to a faster growth rate for the PM. The PM has a statistically significant lower yield of acetate, $Y_{A/S}$, but the yield of ethanol, $Y_{E/S}$, is similar between the two strains. This difference might be caused by the mutation in the non-coding region upstream of the Cthe_0422-3 operon which encodes the Rex (redox) repressor and adhE (Linville et al., submitted for publication; Wietzke and Bahl, 2012). This may cause a switch from acetic acid production to ethanol production which would further help to balance the electron flux in the cell (Linville et al., submitted for publication). Controlling for pH, as was done on these fermentations, allows for a better metabolic flux distribution by reducing the effect of acid formation (Song et al., 2011).

Experiments with *Populus* hydrolysate could be modeled using the same Monod model adapted to include a general unit-less inhibition factor $K_{I,gen}$ ($0 \leqslant K_{I,gen} \leqslant 1$) as follows:

$$\mu = \mu_{max} * \left(\frac{S}{k_S + S}\right) * K_{I,gen} \tag{8}$$

Inhibition terms that were dependent on the concentration of the *Populus* hydrolysate or of individual inhibitors were not found to describe the data well. The WT and PM strains have the ability to degrade two of the inhibitors in the hydrolysate that can be easily monitored during the growth period: furfural and HMF (Boyer et al., 1992; Palmqvist et al., 1999). The furfural reduction rate has been shown to increase with increasing specific growth rate and increasing furfural concentrations (Palmqvist and Hahn-Hagerdal, 2000b). Therefore, degradation was modeled as a pseudo-second order rate equation by being a first order equation with respect to both inhibitor concentration and biomass as follows:

$$\frac{dI_{HMF}}{dt} = -k_{I,HMF} * I_{HMF} * X \tag{9}$$

$$\frac{dI_F}{dt} = -k_{I,F} * I_F * X \tag{10}$$

where I_{HMF} and I_F are the inhibitor concentrations of HMF and furfural, respectively (g/L); and $k_{I,HMF}$ and $k_{I,F}$ are the kinetic constants for each compound (L/g h). The matrix of model parameters from the standard condition optimized model was supplied to the *Populus* hydrolysate model along with a new matrix of guessed values of

Table 1
Optimal parameter estimates for Monod model in standard conditions and hydrolysate.

	μ_{max} (h^{-1})	K_S (g/L)	$Y_{X/S}$ (g/g)	$Y_{E/S}$ (g/g)	$Y_{A/S}$ (g/g)	$K_{I,gen}$ (h^{-1})	$K_{I,HMF}$	$K_{I,F}$	R^2
WT in 0% hydrolysate	0.571 ± 0.007	0.915 ± 0.044	0.234 ± 0.002	0.067 ± 0.004	0.273 ± 0.002	–	–	–	0.995
WT in 10% hydrolysate	0.571 ± 0.007	0.915 ± 0.044	0.234 ± 0.002	0.097 ± 0.008	0.330 ± 0.027	0.757 ± 0.003	2.020 ± 0.060	11.057 ± 1.159	0.968
PM in 0% hydrolysate	1.223 ± 0.029	2.217 ± 0.094	0.244 ± 0.008	0.088 ± 0.003	0.254 ± 0.009	–	–	–	0.972
PM in 10% hydrolysate	1.223 ± 0.029	2.217 ± 0.094	0.244 ± 0.008	0.109 ± 0.009	0.308 ± 0.009	0.991 ± 0.003	2.060 ± 0.152	8.826 ± 0.683	0.979
PM in 17.5% hydrolysate	1.223 ± 0.029	2.217 ± 0.094	0.244 ± 0.008	0.119 ± 0.004	0.436 ± 0.015	0.888 ± 0.002	2.131 ± 0.028	10.565 ± 0.112	0.952

inhibition parameters. The parameters were optimized in a similar manner where the weighted least square errors of the six variables (biomass, substrate, ethanol, acetate, HMF, and furfural) were minimized. When the Monod parameters were held constant, the model consistently under predicted the formation of end products; therefore, the model was also adjusted to allow for possible changes in product yields. All other model parameters estimated from the 0% v/v *Populus* hydrolysate experiments (μ_{max}, k_S, and $Y_{X/S}$) were held constant.

The optimal parameters estimated for the *Populus* hydrolysate conditions are shown in Table 1 and the model-calculated profiles for the WT and PM strains using these parameters are shown in Fig. 2. The model accurately describes the experimental data based on the R^2 value for the entire system (Table 1). Less inhibition is indicated as values of $k_{I,gen}$, increase. As to be expected, the WT in 10% v/v *Populus* hydrolysate is the most inhibited, followed by the PM in 17.5% v/v *Populus* hydrolysate, and PM in 10% v/v *Populus* hydrolysate. The degradation rate constants $k_{I,HMF}$ and $k_{I,F}$ are very similar for the WT and PM (Table 1) which suggests that the PM does not have a greater ability to detoxify the hydrolysate. The initial concentration of furfural and HMF were similar for the WT and PM strains. However, comparison of the lag time in biomass growth versus the degradation of the inhibitors for the WT and PM further suggests that the WT dedicates more resources to the degradation of furfural and HMF than the PM does. Both the WT and PM reach the exponential growth phase 6 h into the fermentation. At the end of the lag phase, the WT in 10% v/v *Populus* hydrolysate has degraded 40% of the furfural and 12% of the HMF. The PM in 10% v/v *Populus* hydrolysate only degraded 12% of the furfural and 5% of the HMF in the lag phase. In 17.5% v/v *Populus* hydrolysate, the PM degrades 23% of the furfural and 7% of the HMF by the end of the lag phase. Furthermore, the WT in 10% v/v *Populus* hydrolysate does not reach a biomass concentration of greater than 0.1 g/L until approximately 4.6 h after it reaches the exponential growth phase (10.6 h total fermentation time); at that point 90% of the furfural and 71% of the HMF have been degraded. The PM reaches a biomass concentration of greater than 0.1 g/L in approximately 3.25 and 3.5 h after it reaches the exponential growth phase in 10% and 17.5% v/v *Populus* hydrolysate (9.25 and 9.5 h total fermentation time), respectively. At approximately 3.25 h into the exponential growth phase, the PM has only degraded 68% of the furfural and 23% of the HMF in 10% v/v *Populus* hydrolysate, and 81% of the furfural and 27% of the HMF in 17.5% v/v *Populus* hydrolysate. Similarly, increased furfural tolerance in an *Escherichia. coli* EMFR9 strain was accompanied by a decrease in the rate of furfural reduction in vivo and a decrease in the NADPH-dependent furfural reductase activity in vivo (Miller et al., 2009). Reducing the NADPH-dependent furfural reducase activity permitted increased growth in the presence of furfural by slowing the depletion of NADPH that is required for biosynthesis (Miller et al., 2009).

Furthermore, furfural and HMF directly inhibit adhE, resulting in NAD(P)H depletion due to their reduction to their corresponding alcohols thereby affecting glycolysis and TCA fluxes (Almeida et al., 2007; He et al., 2012; Zhang et al., 2011). The PM has a mutation in the non-coding region upstream of the Cthe_0422-3 operon which encodes the Rex (redox) repressor and adhE (Linville et al., submitted for publication). The mutation resulted in a slightly higher expression level of both genes in all test conditions for the PM

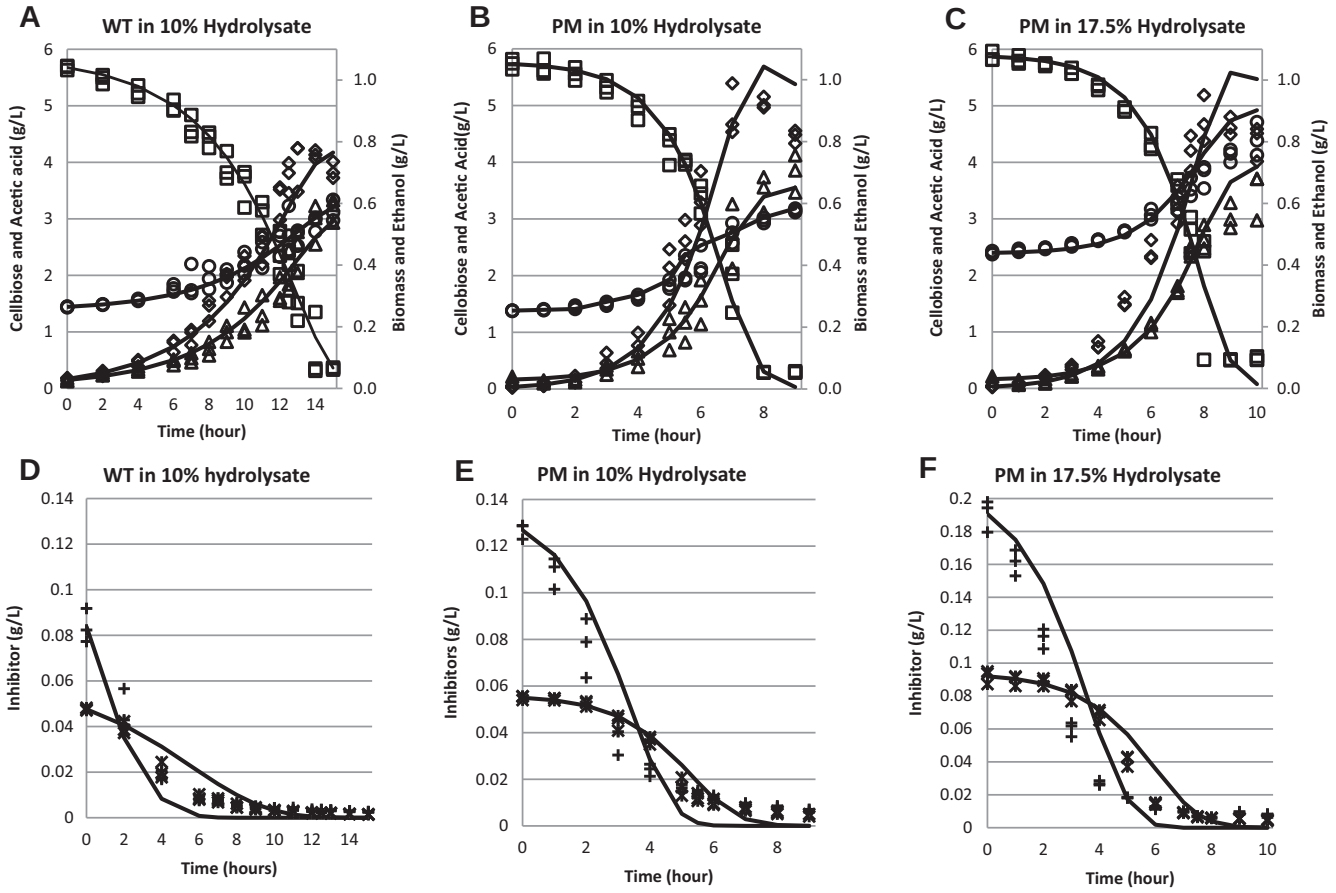

Fig. 2. The model-calculated and experimental results for the (A) WT in 10% v/v *Populus* hydrolysate, (B) PM in 10% v/v *Populus* hydrolysate and (C) PM in 17.5% v/v *Populus* hydrolysate for cellobiose utilization ([]), biomass formation (◇), and ethanol (Δ), and acetic acid (o) production. The estimated and experimental results for (D) WT in 10% v/v *Populus* hydrolysate, (E) PM in 10% v/v *Populus* hydrolysate, and (F) PM in 17.5% v/v *Populus* hydrolysate for furfural (+) and HMF (*). Experimental data are represented by points; model results are represented by solid lines.

whereas the WT had significant decreased expression of these genes in *Populus* hydrolysate media (Linville et al., submitted for publication). Therefore, it is surprising that both strains similarly increased the ethanol yield in the *Populus* hydrolysate conditions (Table 1). Comparative proteomics indicate that the central carbon metabolism, levels of alcohol dehydrogenase, the redox balance, and other general stress responses are needed to tolerate furfural inhibition (He et al., 2012). The increased ethanol production for the WT may be due to the need to balance the electron flow while converting the furfural and HMF into their corresponding alcohols. However, since the WT lacks the mutation of the PM, the increased ethanol may come at the expense of other cellular functions. The PM strain also has a number of mutations affecting genes related to DNA repair (Cthe_2376), and RNA transcription (Cthe_2724), translation (Cthe_2727) and degradation (Cthe_0158) (Linville et al., submitted for publication). These mutations may increase the tolerance of the PM strain to the inhibitory compounds found in the *Populus* hydrolysate or may contribute to faster growth of the PM through energy conservation.

The codependence between the optimized parameters, as shown by their correlation, was determined from the covariance matrix. The correlation matrix for the WT in 0% and 10% v/v *Populus* hydrolysate can be seen in Table 2. The maximum specific growth rate, μ_{max}, the half saturation constant, k_S, and the yield of ethanol, $Y_{E/S}$, are all strongly correlated among one another. The parameters in the *Populus* hydrolysate media calculations are less correlated. The furfural degradation constant, k_F, is correlated to the yield of both ethanol, $Y_{E/X}$, and acetate, $Y_{A/S}$. The PM has similar correlation between the parameters for the standard and *Populus* hydrolysate calculations (data not shown).

3.2. Populus hydrolysate tolerance

In order to further determine the inhibitory effects of the hydrolysate, both strains were grown in selected concentrations of *Populus* hydrolysate (0%, 10%, 20%, and 30% v/v *Populus* hydrolysate). Fig. 3 shows the OD_{600} over time. The *Populus* hydrolysate is a dark brown color whose intensity increased with concentration. As the strain grows in the presence of hydrolysate, the color lightens due to degradation of some of the compounds and becomes milky as the biomass increases. This color change accounts for the negative OD_{600} seen at the higher concentrations of hydrolysate. For any given concentration of hydrolysate, the PM has a higher OD_{600} than the WT strain. The largest difference is in standard media (0% v/v *Populus* hydrolysate) with the PM having 3-times greater OD_{600} than the WT strain. The WT strain is completely inhibited at 20% v/v *Populus* hydrolysate whereas the PM strain is completely inhibited at 30% v/v *Populus* hydrolysate.

3.3. Individual inhibitors

In order to determine the inhibition contributed to the hydrolysate by the individual compounds, both the WT and PM strain of *C. thermocellum* were grown in six individual inhibitors (furfural, HMF, syringic acid, vanillin, galacturonic acid, and hydroxybenzoic acid) at concentrations equal to those found in media containing 17.5% and 35% v/v *Populus* hydrolysate. The six inhibitors were combined to make a model hydrolysate representative of the 17.5% v/v and 35% v/v concentrations. Table 3 lists the concentrations of individual and combined inhibitors in the media. Samples were taken at 12, 24 and 48 h after inoculation. The optical density, cellobiose consumption, and ethanol and acetic acid production at each time point are shown in Fig. 4. Overall, the PM is less inhibited in all conditions than the WT strain as demonstrated by its greater OD_{600} (Fig. 4A), cellobiose consumption (Fig. 4B), and ethanol production (Fig. 4C). However, the PM strain produced roughly the same amount of acetic acid (Fig. 4D), which could be due to mutations in the PM strain in the non-coding region upstream of Cthe_0442-3 as discussed above (Linville et al., submitted for publication). There is no significant reduction (less than 10%) in OD_{600} for the PM in the furfural, HMF, or syringic acid conditions when compared to the OD_{600} of the PM in standard medium based on the average maximum value over the time course (Fig. 4A). Also, there is no significant reduction in OD_{600} for the model or actual 17.5% v/v hydrolysate conditions. There is a slight reduction (10–25%) in OD_{600} in both vanillin and the lower concentration of galacturonic acid, moderate reduction (25–75%) in OD_{600} for the lower concentration of 4-hydroxybenzonic acid and the 35% v/v model hydrolysate, and sever reduction (greater than 75%) in the higher concentration of galacturonic acid and 4-hydrolxybenzoic acid. For the WT strain, furfural, HMF, syringic acid, vanillin and

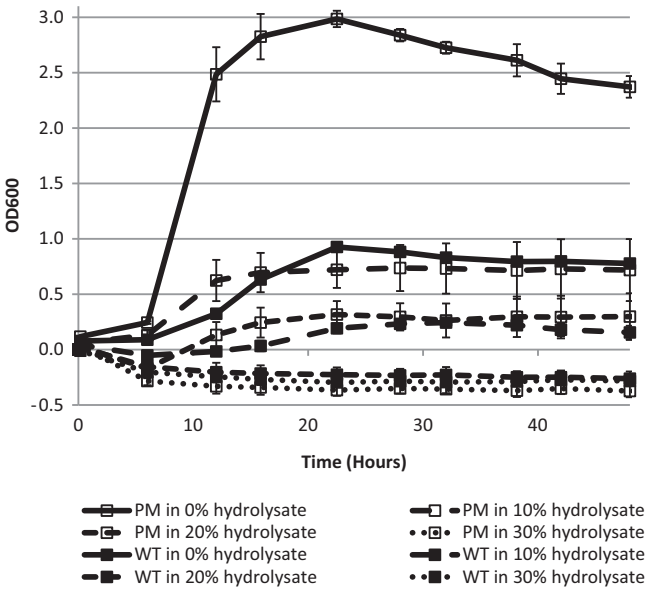

Fig. 3. OD_{600} of the PM ([]) and WT (■). Solid line is 0% v/v *Populus* hydrolysate, long dash line is 10% v/v *Populus* hydrolysate, short dash line is 20% v/v *Populus* hydrolysate and dotted line is 30% v/v *Populus* hydrolysate. Error bars represent standard deviation of triplicate results.

Table 2
Correlation matrix for optimized parameters of the WT in 0% and 10% hydrolysate media showing strong correlation between a number of parameters. The PM has similar correlations between the optimized parameters (data not shown).

WT in 0% hydrolysate						WT in 10% hydrolysate					
	μ_{max}	K_S	$Y_{X/S}$	$Y_{E/X}$	$Y_{A/X}$		$K_{I,HMF}$	$K_{I,F}$	$K_{I,gen}$	$Y_{E/X}$	$Y_{A/X}$
μ_{max}	1.00	0.90	0.36	−0.93	−0.08	$K_{I,HMF}$	1.00	−0.22	−0.26	−0.03	−0.04
K_S	0.90	1.00	0.16	−0.98	0.13	$K_{I,F}$	−0.22	1.00	0.19	−0.60	−0.65
$Y_{X/S}$	0.36	0.16	1.00	−0.32	0.01	$K_{I,gen}$	−0.26	0.19	1.00	−0.10	−0.12
$Y_{E/X}$	−0.93	−0.98	−0.32	1.00	−0.18	$Y_{E/X}$	−0.03	−0.60	−0.10	1.00	−0.16
$Y_{A/X}$	−0.08	0.13	0.01	−0.18	1.00	$Y_{A/X}$	−0.04	−0.65	−0.12	−0.16	1.00

Table 3
Concentrations of individual inhibitors representing 17.5% and 35% v/v *Populus* hydrolysate, combined inhibitor concentration for 17.5% and 35% v/v model hydrolysate and the actual concentration in 17.5% v/v *Populus* hydrolysate where used to determine the toxicity of the individual compounds. GA is galacturonic acid and HBA is 4-hydroxybenzoic acid.

	Cellobiose (g/L)	Glucose (g/L)	Furfural (mg/L)	HMF (mg/L)	Syringic acid (mg/L)	Vanillin (mg/L)	GA (g/L)	HBA (g/L)
0% *Populus* Hydrolysate	4.97	0.04						
150 mg/L Furfural	4.66	0.02	108.6					
300 mg/L Furfural	4.67	0.02	233.8					
75 mg/L HMF	4.81	0.02		67.6				
150 mg/L HMF	4.75	0.03		136.0				
50 mg/L Syringic acid	5.38	0.02			50.4			
75 mg/L Syringic acid	4.90	0.02			73.0			
25 mg/L Vanillin	4.61	0.02				24.2		
50 mg/L Vanillin	4.77	0.02				50.4		
2 g/L GA*	5.23	0.03					2.2	
4 g/L GA*	5.55	0.06					4.3	
1.5 g/L HBA*	5.14	0.03						1.7
3 g/L HBA*	4.37	0.03						2.8
17.5% v/v Model hydrolysate	6.24	4.02	165.5	54.8	50.0	25.0	2.6	1.9
35% v/v Model hydrolysate	7.46	7.82	314.8	121.6	75.0	50.0	4.5	3.6
17.5% v/v *Populus* hydrolysate	5.98	3.98	193.6	78.5	40.0	15.0	1.1	0.2

the 17.5% v/v model hydrolysate all caused similar moderate reductions in OD_{600}. There is also moderate reduction in OD_{600} for the lower concentrations of galacturonic acid. There is severe reduction in growth for both hydroxylbenzoic acid concentrations, the higher concentration of galacturonic acid, the 35% v/v model hydrolysate, and the 17.5% v/v *Populus* hydrolysate.

Both the WT and PM strain may be able to grow better in the model hydrolysate than the galacturonic acid and 4-hydroxybenzoic acid conditions likely because the solution was neutralized to a pH of 7.0 in the model hydrolysate before the addition of the other media components. The pH of the media has been shown to have a significant effect on the growth of the culture (Song et al., 2011). Furthermore, based of the growth of the WT in the 17.5% v/v model hydrolysate and actual hydrolysate, the six inhibitors chosen do not represent the full inhibitory effect of the hydrolysate. Similar trends were seen in the cellobiose consumption and ethanol production (Fig. 4B and C, respectively). The PM consumes the smallest amount of cellobiose per unit growth in the 17.5% v/v

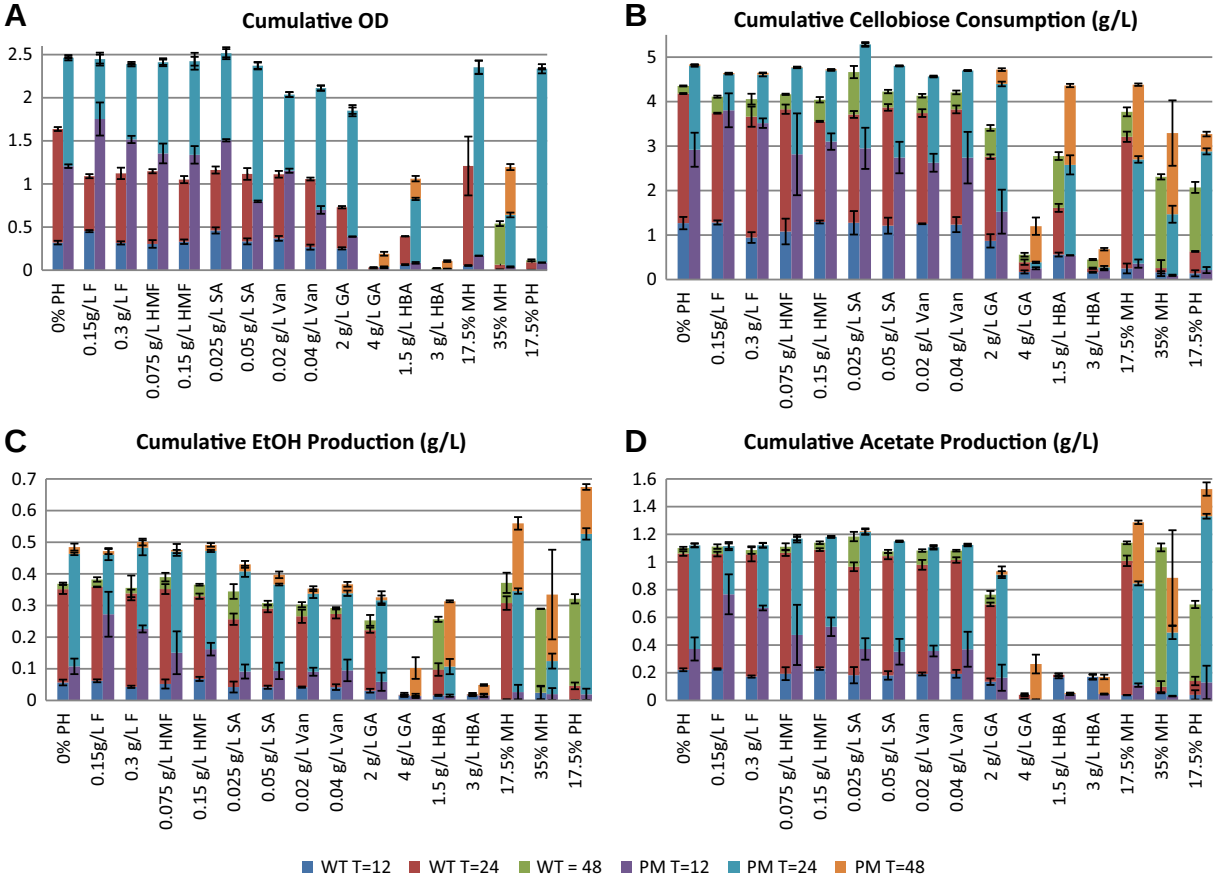

Fig. 4. Effect of various inhibitors on fermentation. For each inhibitor, stacked bars represent cumulative consumption or production at 12, 24, and 48 h. (A) OD_{600}, (B) cellobiose consumption, (C) ethanol production, (D) acetate production.

Populus hydrolysate. One possible explanation is that the *Populus* hydrolysate triggers a stress response in which non-essential pathways are turned off to conserve energy. The highest amount of ethanol and acetic acid produced was in the 17.5% v/v *Populus* hydrolysate followed by the 17.5% v/v model hydrolysate concentrations. Although, the cellobiose consumption is low, the high ethanol and acetic production could be triggered by the need to balance the electron flow to increase the availability of ATP as the cell responds to the inhibitors in the hydrolysate (Linville et al., submitted for publication). The WT strain lacks the ability to increase ethanol and acetic acid production under these conditions which may explain its greater level of inhibition.

3.4. Detoxification

Biotransformation of the inhibitory compounds in the hydrolysate (detoxification) was investigated as a mechanism of tolerance by re-growth experiments in which the PM and WT strains were grown in media reused from earlier fermentation experiments. The initial hydrolysate media ($T = 0$) contained 5.9 g/L cellobiose, 4.1 g/L glucose and 5 g/L acetic acid. Of the various inhibitors, the two that can be most readily measured by HPLC are furfural and HMF with initial concentrations of 58 and 163 mg/L, respectively. During the 72 h preparatory fermentation the PM strain utilized 3.7 g/L cellobiose and 2.4 g/L glucose and produced 0.14 g/L lactic acid, 0.76 g/L ethanol and 3.38 g/L acetic acid. However, the WT strain utilized only 1.9 g/L cellobiose and 0.9 g/L glucose and produced 0.1 g/L lactic acid, 0.25 g/L ethanol and 1.46 g/L acetic acid. Both strains degraded almost all of the furfural and 5-HMF present in the hydrolysate. The cells were removed via filter sterilization with a 0.2 μm filter and the metabolites were adjusted to roughly the same concentration; 3.75 g/L cellobiose, 2.86 g/L glucose, 0.09 g/L lactic acid, and 0.47 g/L ethanol. The acetic acid concentration was not adjusted. Both the WT and PM strains were grown in the adjusted media detoxified by either the WT or PM strain. Fig. 5A–D shows the cell growth, glucan utilization, ethanol production, and acetic acid production over time for each of the four regrowth experiments. The initial ethanol and acetic acid concentrations were subtracted from the final concentrations measured at the end of the experiment for better comparison. Neither strain produced significant concentrations of lactic acid. The fermentation profiles of both strains showed very little dependence on the type of media (WT-detoxified or PM-detoxified) used for the regrowth experiment. The PM had approximately twice the maximum optical density of the WT strain and reached it sooner (15 h compared to 24 h). Furthermore, in both conditions the PM utilized approximately 2.9 g/L cellobiose, 2.1 g/L glucose and produced 0.73 g/L ethanol and 3.0 g/L acetic acid. The WT strain utilized 2.7 g/L cellobiose but only 0.2 g/L glucose and produced 0.35 g/L ethanol and 1.8 g/L acetic acid. The WT strain performed better in the detoxified hydrolysate than in 17.5% v/v *Populus* hydrolysate; however, the PM did not (data not shown). This may be due to the higher acetic acid concentration in the PM detoxified media. The results show that the PM does not have a better ability to detoxify the hydrolysate and that this is not the primary mechanism of tolerance.

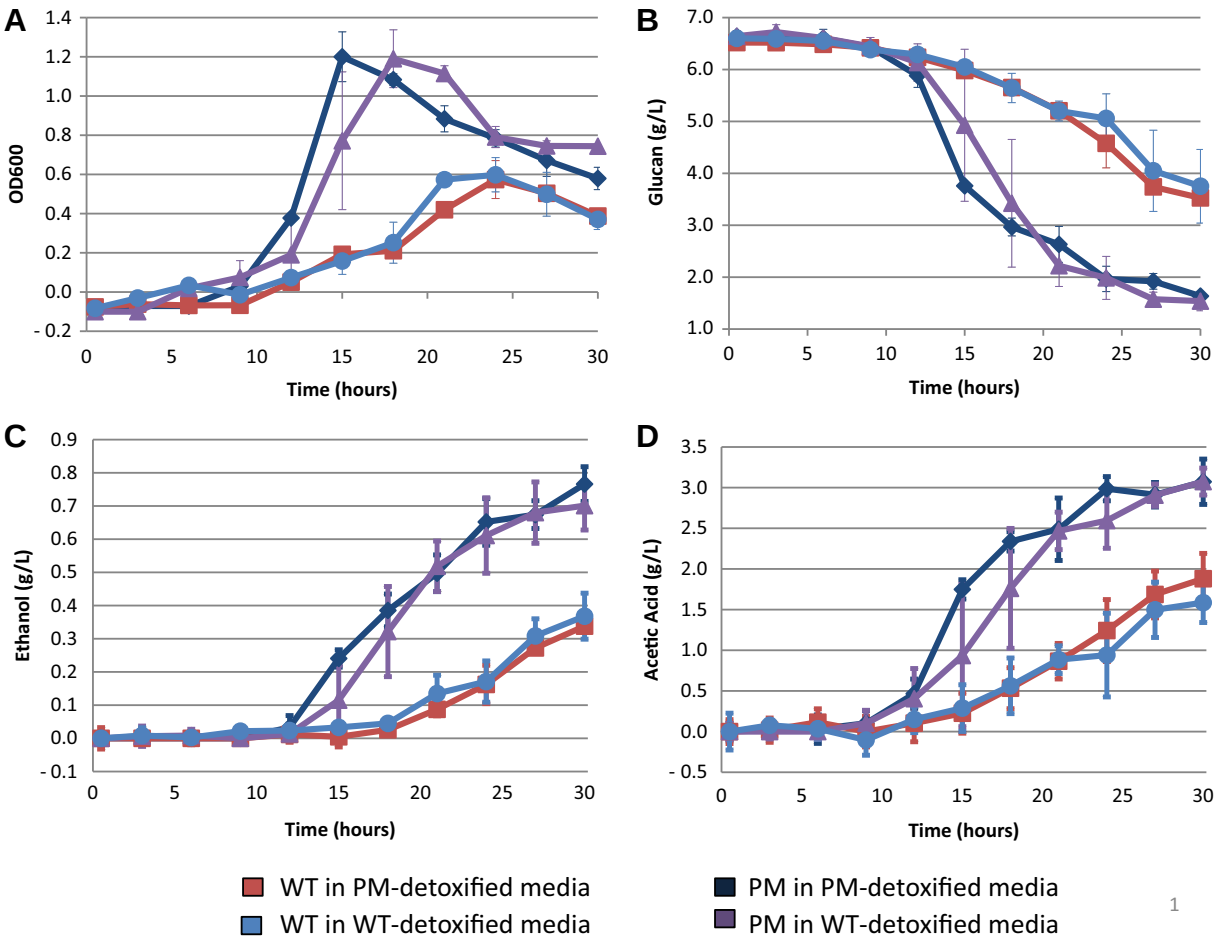

Fig. 5. Results of the re-growth detoxification experiments (A) biomass growth shown as OD_{600}, (B) glucan utilization, (C) ethanol and (D) acetic acid production showing equal detoxification for the WT and PM strain.

4. Conclusions

The results from batch fermentations of *C. thermocellum* on cellobiose were successfully simulated using Monod kinetics. The PM had a higher maximum growth rate and was less inhibited by the hydrolysate than the WT strain; furthermore, the PM is less inhibited by individual compounds than the WT strain. This study also found that the PM does not have a greater ability to detoxify the *Populus* hydrolysate than the WT. Therefore, the increased tolerance to the hydrolysate is apparently due to the combined effects of several mutations in the PM that increased its growth rate (Linville et al., submitted for publication).

Funding statement

This research was supported by the BioEnergy Science Center, a Department of Energy Bioenergy Research Center supported by the Office of Biological and Environmental Research in the Department of Energy Office of Science. Additional support was provided by the Institute for a Secure and Sustainable Environment at the University of Tennessee. Oak Ridge National Laboratory is managed by UT-Battelle, LLC, for the DOE under Contract DE-AC05-00OR22725. The funders had no role in study design, data collection and analysis, decision to publish, or preparation of the manuscript.

Competing Interest Statement

CDC has a financial interest (stock ownership) in Renmatix, Inc. CDC is the Director of the Institute for a Secure and Sustainable Environment which provided funding to support JLL through institutional funds that he has been entrusted to administer.

References

Almeida, J.R.M., Modig, T., Petersson, A., Hahn-Hagerdal, B., Liden, G., Gorwa-Grauslund, M.F., 2007. Increased tolerance and conversion of inhibitors in lignocellulosic hydrolysates by *Saccharomyces cerevisiae*. Journal of Chemical Technology and Biotechnology 82 (4), 340–349.

Baskaran, S., Ahn, H.J., Lynd, L.R., 1995. Investigation of the ethanol tolerance of *Clostridium-thermosaccharolyticum* in continuous-culture. Biotechnology Progress 11 (3), 276–281.

Bouguettoucha, A., Balannec, B., Amrane, A., 2011. Unstructured models for lactic acid fermentation–a review. Food Technology and Biotechnology 49 (1), 3–12.

Boyer, L.J., Vega, J.L., Klasson, K.T., Clausen, E.C., Gaddy, J.L., 1992. The effects of furfural on ethanol-production by *saccharomyces-cerevisiae* in batch culture. Biomass and Bioenergy 3 (1), 41–48.

Brown, S.D., Guss, A.M., Karpinets, T.V., Parks, J.M., Smolin, N., Yang, S.H., Land, M.L., Klingeman, D.M., Bhandiwad, A., Rodriguez, M., Raman, B., Shao, X.J., Mielenz, J.R., Smith, J.C., Keller, M., Lynd, L.R., 2011. Mutant alcohol dehydrogenase leads to improved ethanol tolerance in *Clostridium thermocellum*. Proceedings of the National Academy of Sciences of the United States of America 108 (33), 13752–13757.

DOE/SC-0095. 2006. Breaking the biological barriers to cellulosic ethanol: a joint research agenda, U.S. Department of Energy.

Gnanapragasam, G., Senthilkumara, M., Arutchelvan, V., Velayutham, T., Nagarajan, S., 2011. Bio-kinetic analysis on treatment of textile dye wastewater using anaerobic batch reactor. Bioresource Technology 102 (2), 627–632.

He, M.X., Wu, B., Shui, Z.X., Hu, Q.C., Wang, W.G., Tan, F.R., Tang, X.Y., Zhu, Q.L., Pan, K., Li, Q., Su, X.H., 2012. Transcriptome profiling of Zymomonas mobilis under furfural stress. Applied Microbiology and Biotechnology 95 (1), 189–199.

Hoch, J.A., 1993. Regulation of the phosphorelay and the initiation of sporulation in *Bacillus subtilis*. Annual Review of Microbiology 47, 441–465.

Holwerda, E.K., Lynd, L.R., 2013. Testing alternative kinetic models for utilization of crystalline cellulose (avicel) by batch cultures of *Clostridium thermocellum*. Biotechnology and Bioengineering.

Huang, W.H., Wang, F.S., 2010. Kinetic modeling of batch fermentation for mixed-sugar to ethanol production. Journal of the Taiwan Institute of Chemical Engineers 41 (4), 434–439.

Klinke, H.B., Thomsen, A.B., Ahring, B.K., 2004. Inhibition of ethanol-producing yeast and bacteria by degradation products produced during pre-treatment of biomass. Applied Microbiology and Biotechnology 66 (1), 10–26.

Linville, J.L., Rodriguez Jr., M., Land, M., Syed, M.H., Engle, N.L., Tschaplinski, T.J., Mielenz, J.R., Cox, C.D. Submitted. Industrial Robustness: understanding the mechanism of tolerance for the Populus hydrolysate-tolerant mutant strain of Clostridium thermocellum. Plos One

Ljunggren, M., Willquist, K., Zacchi, G., van Niel, E.W.J., 2011. A kinetic model for quantitative evaluation of the effect of hydrogen and osmolarity on hydrogen production by *Caldicellulosiruptor saccharolyticus*. Biotechnology for Biofuels 4, 15.

Marquardt, D.W., 1963. An algorithm for least-squares estimation of nonlinear parameters. Journal of the Society for Industrial and Applied Mathematics 11 (2), 431–441.

Miller, E.N., Jarboe, L.R., Turner, P.C., Pharkya, P., Yomano, L.P., York, S.W., Nunn, D., Shanmugam, K.T., Ingram, L.O., 2009. Furfural inhibits growth by limiting sulfur assimilation in ethanologenic *Escherichia coli* strain LY180. Applied and Environmental Microbiology 75 (19), 6132–6141.

Ozkan, M., Desai, S.G., Zhang, Y., Stevenson, D.M., Beane, J., White, E.A., Guerinot, M.L., Lynd, L.R., 2001. Characterization of 13 newly isolated strains of anaerobic, cellulolytic, thermophilic bacteria. Journal of Industrial Microbiology and Biotechnology 27 (5), 275–280.

Palmqvist, E., Almeida, J.S., Hahn-Hagerdal, B., 1999. Influence of furfural on anaerobic glycolytic kinetics of *Saccharomyces cerevisiae* in batch culture. Biotechnology and Bioengineering 62 (4), 447–454.

Palmqvist, E., Hahn-Hagerdal, B., 2000a. Fermentation of lignocellulosic hydrolysates. I: inhibition and detoxification. Bioresource Technology 74 (1), 17–24.

Palmqvist, E., Hahn-Hagerdal, B., 2000b. Fermentation of lignocellulosic hydrolysates. II: inhibitors and mechanisms of inhibition. Bioresource Technology 74 (1), 25–33.

Pienkos, P.T., Zhang, M., 2009. Role of pretreatment and conditioning processes on toxicity of lignocellulosic biomass hydrolysates. Cellulose 16 (4), 743–762.

Raman, B., McKeown, C.K., Rodriguez, M., Brown, S.D., Mielenz, J.R., 2011. Transcriptomic analysis of *Clostridium thermocellum* ATCC 27405 cellulose fermentation. Bmc Microbiology 11, 15.

Riederer, A., Takasuka, T.E., Makino, S., Stevenson, D.M., Bukhman, Y.V., Elsen, N.L., Fox, B.G., 2011. Global gene expression patterns in *Clostridium thermocellum* as determined by microarray analysis of chemostat cultures on cellulose or cellobiose. Applied and Environmental Microbiology 77 (4), 1243–1253.

Roberts, S.B., Gowen, C.M., Brooks, J.P., Fong, S.S., 2010. Genome-scale metabolic analysis of *Clostridium thermocellum* for bioethanol production. Bmc Systems Biology 4, 31.

Schell, D.J., Farmer, J., Newman, M., McMillan, J.D., 2003. Dilute-sulfuric acid pretreatment of corn stover in pilot-scale reactor–investigation of yields, kinetics, and enzymatic digestibilities of solids. Applied Biochemistry and Biotechnology 105, 69–85.

Shao, X.J., Lynd, L., 2013. Kinetic modeling of xylan hydrolysis in co- and countercurrent liquid hot water flow-through pretreatments. Bioresource Technology 130, 117–124.

Shuler, M.L., Kargi, F., 2002. Bioprocess Engineering: Basic Concepts, Second ed. Prentice Hall PTR, Upper Saddle River, NJ.

Song, J.X., An, D., Ren, N.Q., Zhang, Y.M., Chen, Y., 2011. Effects of pH and ORP on microbial ecology and kinetics for hydrogen production in continuously dark fermentation. Bioresource Technology 102 (23), 10875–10880.

Wietzke, M., Bahl, H., 2012. The redox-sensing protein Rex, a transcriptional regulator of solventogenesis in *Clostridium acetobutylicum*. Applied Microbiology and Biotechnology 96 (3), 749–761.

Williams, T.I., Combs, J.C., Lynn, B.C., Strobel, H.J., 2007. Proteomic profile changes in membranes of ethanol-tolerant *Clostridium thermocellum*. Applied Microbiology and Biotechnology 74 (2), 422–432.

Yu, T.T., Xu, X.P., Peng, Y.F., Luo, Y.M., Yang, K.Q., 2012. Cell wall proteome of *Clostridium thermocellum* and detection of glycoproteins. Microbiological Research 167 (6), 364–371.

Zhang, Y., Han, B., Chukwuemeka Ezeji, T., 2011. Biotransformation of furfural and 5-hydroxymethylfurfural (HMF) by *Clostridium acetobutylicum* ATCC 824 during butanol fermentation. New Biotechnology 29 (3), 345–354.

Zhang, Y.H., Lynd, L.R., 2003. Quantification of cell and cellulase mass concentrations during anaerobic cellulose fermentation: Development of an enzyme-linked immunosorbent assay-based method with application to *Clostridium thermocellum* batch cultures. Analytical Chemistry 75 (2), 219–227.